Taylor & Francis
Taylor & Francis Group

Automatika

Journal for Control, Measurement, Electronics, Computing and Communications

ISSN: (Print) (Online) Journal homepage: www.tandfonline.com/journals/taut20

Monitoring the condition of nitrogen-filled tires using weightless neural networks

Avantika Rattan, Naveen Venkatesh S, V. Sugumaran & P. S. Anoop

To cite this article: Avantika Rattan, Naveen Venkatesh S, V. Sugumaran & P. S. Anoop (2024) Monitoring the condition of nitrogen-filled tires using weightless neural networks, Automatika, 65:2, 523-537, DOI: 10.1080/00051144.2024.2310979

To link to this article: https://doi.org/10.1080/00051144.2024.2310979

Published online: 11 Feb 2024.

AUTOMATIKA
2024, VOL. 65, NO. 2, 523–537
https://doi.org/10.1080/00051144.2024.2310979

Monitoring the condition of nitrogen-filled tires using weightless neural networks

Avantika Rattan, Naveen Venkatesh S*, V. Sugumaran and P. S. Anoop**

School of Mechanical Engineering (SMEC), Vellore Institute of Technology, Chennai, India

ABSTRACT

The novelty of this paper revolves around monitoring the condition of nitrogen-filled tires through the fusion of features and utilization of weightless neural networks. A tire pressure monitoring system (TPMS) plays a crucial role in ensuring vehicle safety and comfort. Reckless driving, poor road conditions, continual operation, higher road friction and excessive load are certain factors that can degrade the longevity of tires. Such conditions can result in instantaneous fault attacks in tires raising a concern for safety and comfort. To apply instantaneous and accurate fault diagnosis, the present study leverages machine learning techniques through the integration of an adaptive and robust algorithm, namely, the Wilkes, Stonham and Aleksander Recognition Device (WiSARD) classifier. The experiment uses three types of features namely, statistical, histogram and autoregressive moving average (ARMA) features. The J48 decision tree algorithm was used to pinpoint the key attributes crucial for classification. Following this, the identified attributes were segregated into training and testing datasets, facilitating the evaluation of the WiSARD classifier. Hyperparameter tuning was carried out to achieve optimal value for maximizing classification accuracy and minimizing computational time. Among the features considered, ARMA features delivered the best test set accuracy of about 96.18%.

ARTICLE HISTORY
Received 3 November 2023
Accepted 23 January 2024

KEYWORDS
Tire pressure monitoring system (TPMS); machine learning; Wilkes, Stonham and Aleksander Recognition Device (WiSARD) classifier; fault diagnosis; hyperparameter

1. Introduction

Transportation is an indispensable cornerstone of civilization growth that facilitates the movement of people and goods across distances with proper speed and comfort. The inexorable need for transportation has spurred technological advancement. The automotive sector has played a pivotal role in reshaping the world and the very transportation infrastructure. However, the rise in the developments inside the automotive sector was instrumented with the invention of tires. Tires act as the contact medium between the road and the vehicle that enables the movement of the vehicle. Additionally, tires are one of the major components that help in sustaining the comfort and safety of vehicle occupants. The possible reasons that can degrade the longevity and reliability of tires include, high rolling friction, dynamic road conditions, forces, moments, reckless driving, varying climatic conditions and improper pressure management [1]. Tires are manufactured in different dimensions and quality to adapt to the use conditions under various weather conditions, terrain locations and performance requirements. Tires are inflated up to a specific pressure such that the vehicle is capable of withstanding the load applied, counteract road shock transmission and impose proper braking. Additionally, the inflation tire pressure varies from vehicle to vehicle depending on the type and application of the vehicle. To improvise manoeuvrability, braking performance and vehicle balance, maintaining the appropriate tire pressure is essential [2]. Furthermore, underinflated or overinflated tires can lead to deprived vehicle performance and useful tire life. Poor tire maintenance leads to a flat tire, blowout and ultimately crashes. A tire pressure monitoring system (TPMS) helps in monitoring the air pressure in the tire of a vehicle and alerts the driver if pressure is reduced to its threshold value, thereby assisting in accident prevention, extended tire life and improved fuel economy [3].

TPMS is a valuable safety system for vehicles that assists the driver in maintaining the proper pressure in tires. While there are some drawbacks related to TPMS, the benefits typically outweigh [4]. TPMS types include Direct TPMS and Indirect TPMS. Direct TPMS uses sensors that are mounted on the rim (inside the tire) to help in measuring the inflation of each tire separately. On lowering air pressure below 25% from the recommended level, the sensor notifies the computer

CONTACT V. Sugumaran v_sugu@yahoo.com School of Mechanical Engineering (SMEC), Vellore Institute of Technology, Chennai 600127, India
*Present address: Division of Operation and Maintenance Engineering, Luleå University of Technology, Luleå, Sweden
**Present address: Sustainable Mobility Automobile Research Technology (SMART) Center, Dept. of Electronics and Communication Engineering, Amrita Vishwa Vidyapeetham, Amritapuri, India

system which gives a warning signal to the driver [5]. Indirect TPMS works with the anti-locking braking system (ABS) of the vehicle wherein the ABS monitors the wheel speed. A drop in the tire pressure makes the wheel rotate at a varied speed than the counterparts, thereby signifying low tire pressure. TPMS has evolved as a silent deterministic feature of the vehicle with the advancement in technology. Numerous studies have been carried out in the field of TPMS as discussed next. Lee et al. developed and implemented an indirect TPMS within a vehicle suspension system, employing an adaptive extended Kalman filtering approach [6]. Silalahi et al. undertook an extensive investigation into the advancement of tire pressure monitoring systems (TPMS) [7]. This effort built upon the groundwork laid by Hasan et al., in which they intricately integrated essential components, including an RF transmitter, pressure sensor, switch and signal conditioning unit, switch and a robust, high-capacity battery, into the system [8]. Silalahi et al. further enhanced the TPMS by introducing additional elements, specifically a pressure sensor, microcontroller and Bluetooth technology, thereby augmenting the system's capabilities and functionalities. Their work signifies a noteworthy progression in the evolution of TPMS technology.

Pioneering surface-micromachining technology is introduced for the seamless integration of a piezoresistive pressure sensor and an accelerometer aimed at the TPMS [9]. Ralaxumi Rajkumar Patil devised a configuration that entails a wireless MQTT-driven apparatus meticulously crafted for data transmission to a smartphone application, thus empowering remote oversight of tire health across global locations. This set-up facilitates wireless monitoring of tire pressure and temperature, eliminating the necessity for an autonomous sensor reading controller due to the utilization of the ESP8266 [10].

Recent years have observed a marginal rise in the application of machine learning techniques in the field of condition monitoring and fault diagnosis. Machine learning algorithms enjoy widespread acceptance primarily because of their capacity to provide results that are not only accurate and precise but also instantaneously presented. Additionally, the capability of machine learning algorithms to solve complex problems and provide real-time solutions has made them the preferred technique for numerous applications. Table 1 represents the recent research works carried out in monitoring tire pressure using machine learning techniques.

The literature survey carried out above provided some significant insights that are summarized as follows:

- Direct TPMS-based fault diagnosis studies were extensively carried out over indirect TPMS. Also, Direct TPMS was a costly affair.
- The minimal number of tire conditions were classified using conventional techniques.
- Numerous techniques for monitoring tire conditions were observed. However, the use of vibration-based assessments is still unexplored in the field of TPMS.
- Classification of multiple tire conditions using machine learning algorithms is still under development stages.
- The impact of weightless neural networks for the classification of tire conditions has not been performed yet.

Table 1. Literature works carried out in TPMS using machine learning.

References	Methodology
[11]	Emphasizes the detection of faults in vehicles for enhanced safety and optimal maintenance, spotlighting electronic tire pressure control systems.
[12]	Exploration of the interconnectedness between tire pressure, rolling resistance, and fuel consumption, factoring in variables such as vehicle weight, brake utilization and cruise control usage.
[13]	Combination of decision tree and support vector machine (SVM) for the TPMS
[14]	Deep learning method for TPMS
[15]	ML approach onboard tire pressure supervision, integrating MEMS accelerometer and decision tree.
[16]	Statistical features (vibration data), the K star Algorithm
[17]	Seven classification techniques, for effective classification of astronomical objects, providing insights applicable to TPMS.

The present study utilizes weightless neural networks (WNNs) in the form of Wilkes, Stonham and Aleksander Recognition Device (WiSARD) classifier for classifying different conditions of nitrogen-filled tires. WiSARD is a weightless neural model which uses look-up tables to store the function computed by each neuron rather than storing it in the weights of a neuron connection. It is a random-access memory (RAM)-based neural network model. Weightless Neural Networks (WNNs) have versatile applications, prominently in classification, pattern recognition tasks and notably, time-series forecasting [18], data stream clustering [19], robot navigation [20], identification of face features [21], recognition of fingerprints [22] and sorting based on image recognition [23]. Aleksander crafted a novel type of neuron using RAM devices based on the principles of Boolean logic. The learning process for this network occurs through the transmission of truth tables stored in the RAM. Only certain portions of the input pattern are recognized and assimilated by the WNN node. These specific patterns are used to produce an address in the RAM, which is instrumental in establishing a mapping criterion that is then translated into a binary form for input into the network. The research basically helps in the navigation of seminal contributions that have helped galvanize TPMS exploration. A comprehensive analysis of the referenced papers in

Table 1, states the evidence that none of the researchers have inked the WiSARD classifier for monitoring the nitrogen-filled tire conditions. The study involves statistical, autoregressive moving average (ARMA) and histogram features. The utilization of this specific classifier in conjunction with these diverse features has appeared to be an unexplored avenue in the realm of TPMS research. The J48 algorithm was employed in the present study to identify the highly contributing significant features. The selected features were provided as input to the WiSARD classifier post-division of the dataset into training and test sets with a split ratio of 80%:20%. Hyperparameters such as bleach confidence, bleach step, bleach flag, map type, etc., were varied sequentially to determine the optimal value for achieving the highest possible accuracy. The overall contributions presented in this work are detailed below.

1. Vibration readings for four varied states of a tire (high pressure, punctured, normal and idle) were gathered utilizing a budget-friendly MEMS accelerometer sensor fitted on a tire filled with nitrogen.
2. Useful information from the recorded vibration signals was extracted and represented using different types of features, namely, ARMA, statistical and histogram features. Furthermore, the J48 algorithm was applied to detect and represent the most significant features for every individual feature set.
3. Selected features from each set were allocated into training and test groups at an 80% to 20% ratio. These groups were then provided to the WiSARD classifier to determine the classifier's performance in terms of training, validation and testing accuracy.
4. Various hyperparameters were adjusted and explored to assess their influence on the classification precision of the WiSARD classifier. These important hyperparameters included the bit number, bleach confidence, bleach flag, bleach step, type of map and tic number.
5. The optimal values of hyperparameters were determined and the best combination of features with the WiSARD classifier was proposed. State-of-the-art performance comparison was utilized to portray the impact of the WiSARD classifier in identifying tire conditions.

2. Experimental studies

The present section details the adopted experimental setup and procedure involved in performing the condition monitoring in tires with the aid of vibration signals and a WiSARD classifier.

2.1. Experimental setup

A front-wheel drive vehicle was used in the experiment, and vertical vibration data were collected from the rear left wheel axis, which was fitted with a nitrogen-filled pneumatic tyre. The specification of the tyre used in the present study is presented in Figure 1. To capture these vibrations, a waterproof triaxial MEMS accelerometer, specifically the MMA7361L, was employed. This accelerometer had a frequency range from 1 to 400 Hz, a resonance frequency of 6 kHz and a sensitivity of 206 mV/g. It was meticulously positioned on the rear left wheel hub to capture vertical vibrations along the y-axis, which was of paramount significance in the experiment. The positioning of the MEMS sensor within the vehicle is depicted in Figure 2. The complete specification of the MEMS sensor is provided in Table 2.

2.2. Methods of data acquisition

The success of the experiment hinged on a critical data acquisition device (DAQ) responsible for capturing and converting analogue signals from the accelerometer into a digital format. . To accomplish these tasks, the researchers opted for the NI USB-6001, a well-known DAQ device with impressive specifications, as presented in Table 3, boasting 12 input channels, a 14-bit resolution and a high sampling rate of 20 kS/s. To establish a seamless connection between the DAQ device and the computer system, the researchers utilized the NI LabVIEW software interface, specifically version 2013. They took care to ensure the accuracy of recorded data and reduce the impact of external electrical interference by thoughtfully integrating a shield wire into the process of converting analogue accelerometer vibrations into digital signals. The entire workflow was orchestrated through the NI LabVIEW software interface, serving as the conduit that linked the output of the DAQ device to the monitoring computer system. This meticulous setup guaranteed the precise and efficient collection and processing of vertical vibration data originating from the rear left wheel axis of the front-wheel-drive vehicle, equipped with a nitrogen-filled pneumatic tire.

2.3. Experimental procedure

During this study, routine driving conditions were simulated with operational speeds from 10 km/h to 100 km/h. The experimental trials were conducted on the National Highways of India, known for their relatively smooth road surfaces, to assess real-world road performance. The specifications for the analysed vibration signals are represented as follows:

- Sampling Rate: Data were gathered at tire rotation speeds set between a minimum of 10 km/h and a

Figure 1. Overview of pneumatic tire specification.

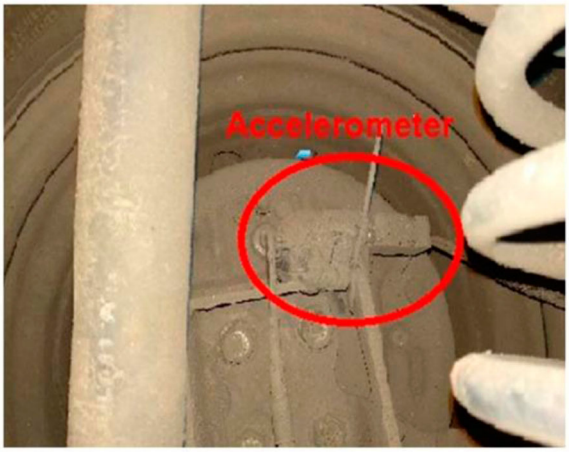

Figure 2. MEMS accelerometer attached to the rear axle of the test vehicle.

Table 2. MEMS accelerometer specification.

Features	Specification
Make	Freescale semiconductor
Weight	< 1 g (accelerometer only) 5 g with supporting electronics
Type	MEMS
Number of axes	3
Description	±1.5 g, ±6 g, Selectable range
Frequency	1–400 Hz (X and Y axis), 1–300 Hz (Z axis)
Resonance frequency	6 kHz (X and Y axis), 3.4 kHz (Z axis)
Sensitivity	800 mV/g @ 1.5 g, 206 mV/g @ 6g
Connector	LGA-14 Package (SMD component)

maximum of 100 km/h. The radius (R) of the 165/80 radial nitrogen-inflated pneumatic tire under study was 30.1 cm. The experiment recorded a maximum signal frequency of 14.73 Hz from the accelerometer, with the lowest frequency measured at 1.47 Hz. Based on the Nyquist Sampling Theorem, the minimum sampling frequency required can be determined as 30 Hz. However, to achieve superior sampling data, a sampling rate of 1 kHz was deemed

Table 3. Data acquisition device (DAQ) specification.

Features	Specification
Make	National Instruments (NI)
Model	NI USB-6001
PC communication	USB
Number of input Channel	4 (Differential), 8 (Single-ended)
ADC type	Successive approximation
ADC resolution	14-bit
Max sampling rate (aggregate)	20kS/S

appropriate and thus chosen for this study. If the sampling frequency is kept below the determined Nyquist frequency, then the frequencies can cross over resulting in aliasing. Also, lower sampling frequencies can create a challenge in signal separation. Thus, an optimal value is affixed.

- Sample Size: To tackle the computational demands of the study encompassing four tire conditions, the fundamental considerations of data availability and consistency are of paramount importance. Consequently, an optimal sample size of 5000 was established.

This study concentrated on analysing a tire that was balanced, which means that no more weight was introduced in addition to the balancing weight (40 g). Data were gathered for high, normal, punctured and idle pressure conditions, among others. In the "Normal" condition, the tire pressure was maintained at the manufacturer's recommended 31 psi (213,737 Pa). To assess this condition, a sequence of experiments was conducted on India's National Highway, strictly adhering to legally imposed speed limits. These tests covered a range of speeds, from 10 km/h to 90 km/h, aimed at evaluating tire performance under typical operational circumstances. Under the "High-pressure" situation, the tire pressure remained at 40 psi (275,790 Pa) and data were obtained through a tri-axial MEMS accelerometer. This data collection occurred within

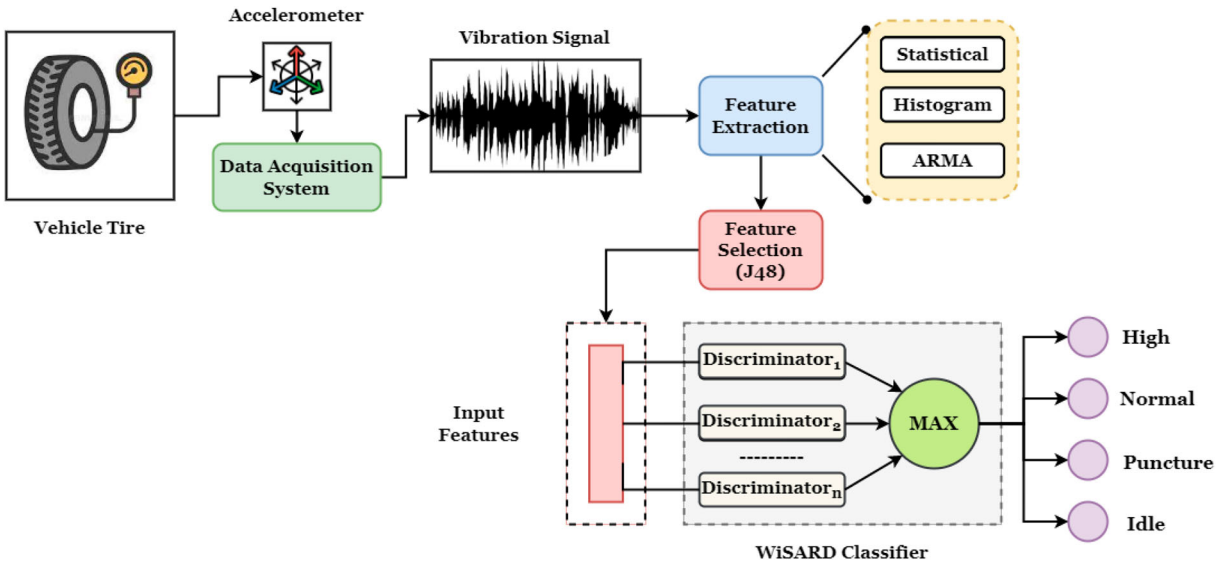

Figure 3. Overall methodology of WiSARD-based monitoring of tire condition.

the same speed range as in previous conditions, all on India's National Highway. To safely replicate the "Punctured" condition, a specific tire pressure of 19 psi (131,000 Pa) was deliberately chosen, with the explicit intent of avoiding zero psi to mitigate potential safety hazards. This aimed to maintain some residual pressure for vehicle stability. The system included an alert to notify the driver when the pressure reached 19 psi (13,1000 Pa), prioritizing safety and simulating real-world puncture conditions. The "Idle" condition involved the collection of vibration signals at a consistent speed of 10 km/h. This choice was made to prevent potential misclassification as signals collected during the "Normal" condition, spanning speeds from 10 km/h to 90 km/h, could lead to misinterpretation.

3. Methodology

The approach for diagnosing tire conditions within the tire condition monitoring system (TCMS) consisted of three key phases: feature extraction, the determination of important features via the J48 algorithm and classification employing the WiSARD classifier. An outline of the complete TCMS fault diagnosis procedure is depicted in Figure 3.

3.1. Feature extraction

Feature extraction is considered one of the fundamental processes in data analysis and machine learning. Feature extraction involves the transformation of raw data into a reduced, manageable set of features which are informative and suitable for training machine learning models. The process of feature extraction serves several purposes that include, computational complexity reduction, model performance improvement and enhancement in the interpretability of the data. The present study utilizes the capability of statistical, histogram and ARMA features to portray the information derived from vibration signals. The description of the features extracted is provided as follows.

- Statistical feature extraction: Descriptive statistical feature analysis of vibration signals will yield a wide set of parameters. A combination of specific parameters can be useful in the extraction of several features such as mean, mode, standard error, kurtosis, skewness, standard deviation, median, sample variances, sum and range (minimum and maximum). These features have been used in diagnosing faults in tires [24]. Here, features such as mean, standard error, median, mode, sample variance and minimum values are only considered. These features could reveal the possible characteristics of the behaviour of the tire includes pressure stability and driving responses to particular pressure variations and scenarios. The mean value states the average pressure maintained within the tire; the standard deviation obtained represents the variability of pressure within the tires. Skewness can reveal the asymmetry in the pressure distribution and kurtosis could reflect the extreme values or outliers, possibly related to sudden drops or spikes.
- Histogram-Based Feature Extraction: Employing histograms for feature extraction involves the organization of discrete and random data into multiple bins. The selection of bins is a pivotal step that relies primarily on two key factors: bin range and bin width. The bin range is determined by dividing the collected data into regular intervals and counting the data points within each interval. Meanwhile, bin width specifies the number of intervals or categories considered. The creation of these bins is based on the range spanning from the minimum to maximum values of amplitudes. A range of bins, spanning from 2 to 100, is generated, and

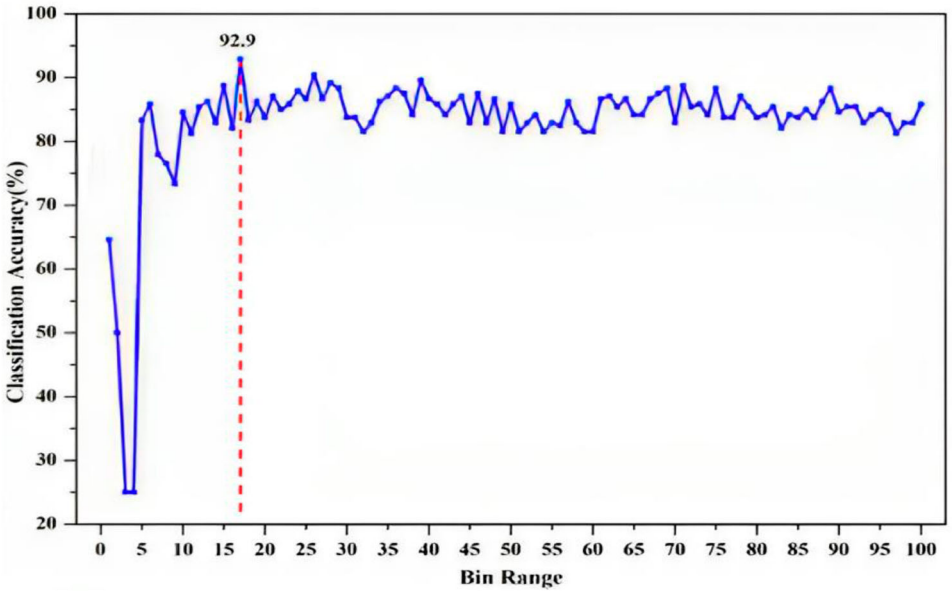

Figure 4. Bin selection for histogram features (bin 17).

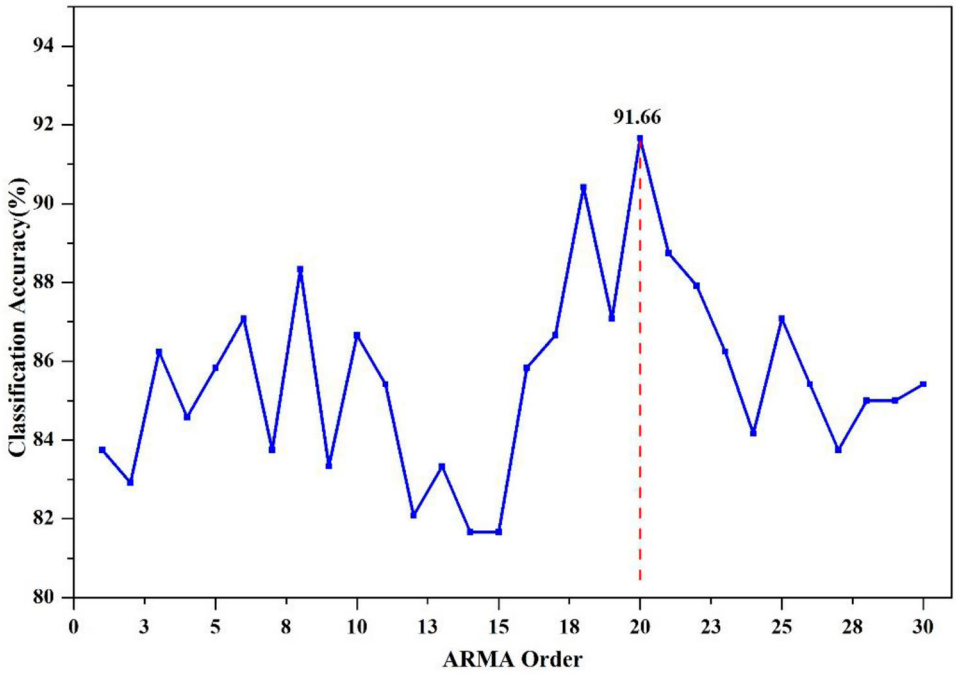

Figure 5. Order selection for ARMA features (order 20).

the associated classification accuracy for each bin is evaluated using the J48 algorithm. Crucial features necessary for fault classification are then identified through the application of the J48 algorithm. In the context of this study, the chosen bin is 17, as depicted in Figure 4.

- Autoregressive moving average (ARMA): Autoregressive moving average (ARMA) is also called a model of anticipation. ARMA applies the concept of both auto-regression and moving average to the time-series data. Any unknown processes with the minimum number of parameters through a time series of the past values can be modelled using ARMA. These past values are fixed as standards to determine the significance of variables to the system. The optimum order value of ARMA (among 30 orders) was determined as 20, as presented in Figure 5.

3.2. Feature selection

Features play a significant role in the process of building a machine-learning model. Feature selection involves selecting a subset of the most informative and relevant features (also known as attributes or variables) from a large set of features for the improvement of model efficiency and performance. Feature selection is particularly salient when dealing with high-dimensional data

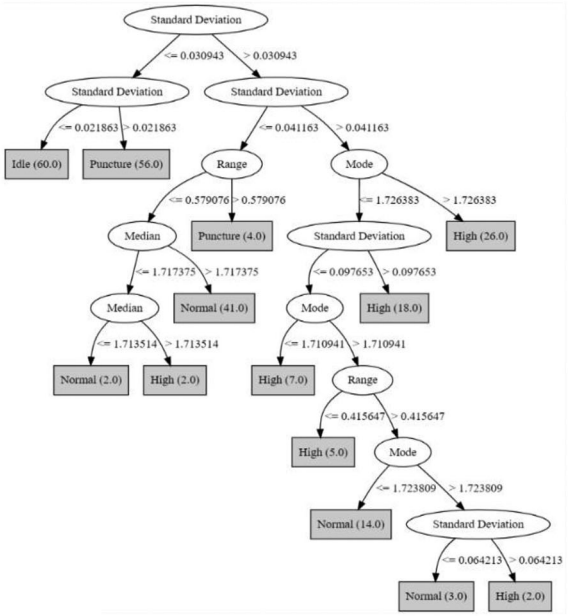

(a) Decision tree for statistical features

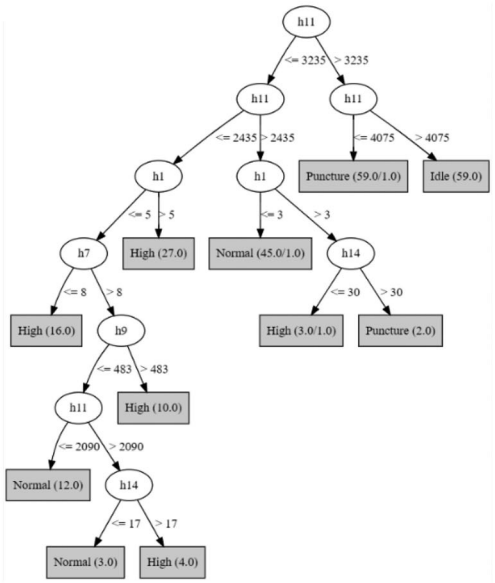

(b) Decision tree for histogram features

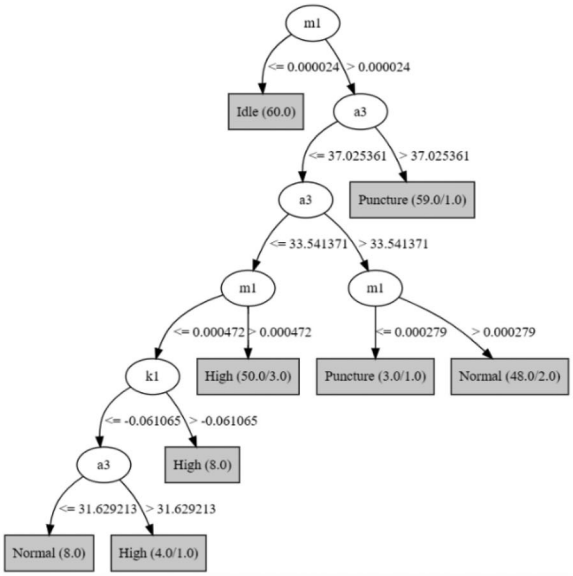

(c) Decision tree for ARMA features

Figure 6. (a) Decision tree for statistical features. (b) Decision tree for histogram features. (c) Decision tree for ARMA features.

as it assists in reducing overfitting, decreases training prediction and enhances model predictability. Feature selection in the present study was performed using the J48 algorithm. The J48 algorithm, a variant of the C4.5 algorithm created by Ross Quinlan and implemented in Java, serves as a decision tree induction technique capable of feature selection. It recursively breaks down a dataset into smaller and uniform subsets. Additionally, it helps in identifying the best attribute for splitting based on maximized information gain and measures reduction in data uncertainty. Employment of the J48 algorithm for feature selection involves the following steps:

1. Data Collection: Assembling a dataset containing both the target variable and the features undergoing selection.
2. Decision Tree Training: Train a decision tree using the J48 algorithm. This process involves repeatedly dividing the datasets based on the most information features.
3. Feature Analysis: Analysing the decision tree to discern which features are used in the first few splits.

The J48 algorithm prioritizes features that frequently appear in the decision tree divisions. These features are

deemed essential for effectively segregating the datasets and can subsequently be chosen for feature selection purposes. The selected features for statistical, histogram and ARMA features are presented in Figure 6(a–c) respectively.

3.3. WiSARD classifier

WiSARD is a weightless neural network model which uses look-up tables to store the function computed by each neuron rather than storing it in the weights of a neuron connection. It is a RAM-based neural network model [25,26]. The noticeable advantages of the WiSARD classifier include the quick execution speed and implementation simplicity. The training of the classifier is a one-shot memorization process that makes the classifier computationally simple compared to the other equation-solving and minimizing methods [27]. Figure 7(a) depicts the core differentiation between weightless and weighted neural networks. Weightless and weighted neural networks employ contrasting approaches in information processing. Weightless networks optimize storage by using RAM to encode features as memory addresses through binary initialization while weighted networks assign weights to features to indicate their significance. Weightless networks excel in data representation and computation, employing memory locations and hashing for efficient operations. On the other hand, weighted networks use synaptic weights for precise signal modulation, which requires more computational resources. Weightless networks are favoured in memory-constrained settings, efficiently storing information and functioning effectively. Figure 7(b) provides a simplified depiction of a RAM network and neuron, illustrating the core components and their interactions.

The RAM device produces binary output, which can take the value 0 or 1. Within Weightless Neural Networks (WNN), the configuration of RAM devices, allows for the implementation of various architectures, with WiSARD being a widely preferred option. The WiSARD structure consists of two or more discriminators, each of which corresponds to a user-defined class. Each discriminator undergoes individual training to learn and recognize patterns associated with its assigned class. Figure 8 offers an overview of the WiSARD classifier, featuring a discriminator module. Inside this discriminator module, RAM devices are assigned the role of mapping the input patterns. These RAM devices analyse and record sub-patterns from the input pattern map, which are depicted in tuple form. During the testing phase, the RAM devices determine the memory address associated with each tuple, providing a stored value of either 0 or 1. Figure 9 delineates the sequential steps within a WiSARD classifier.

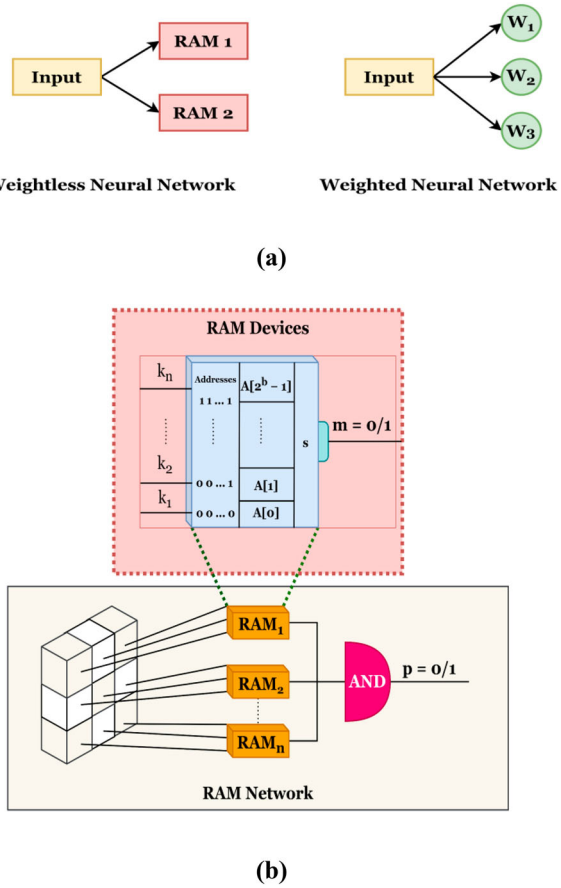

Figure 7. (a) Simple difference among weightless and weighted neural networks. (b) A simplified view of RAM network and neuron (RAM devices).

4. Results and discussion

The performance of the WiSARD classifier in monitoring the condition of nitrogen-filled tires was analysed in the current study. High, puncture, normal and idle are the four tire conditions considered in the study. The classifier performance was evaluated using various hyperparameters such as tic number, map type, bleach flag, bleach confidence and bit number. For the initial assessment, a training set with 80% of the initial data and a test set with 20% of the initial data were formulated. The experimentation was carried out to determine the optimal hyperparameter configuration of the WiSARD classifier for every feature set to obtain superior performance.

4.1. Effect of "bit number"

The Bit number is one of the critical parameters that signifies the number of bits required to constitute across the sparse distributed representation. The resolution and capacity of the classifier is determined by the number of bits. The information in the classifier is represented in the form of binary units thereby termed as bits. WiSARD creates or learns patterns through the collection of randomized bit cells in the binary form.

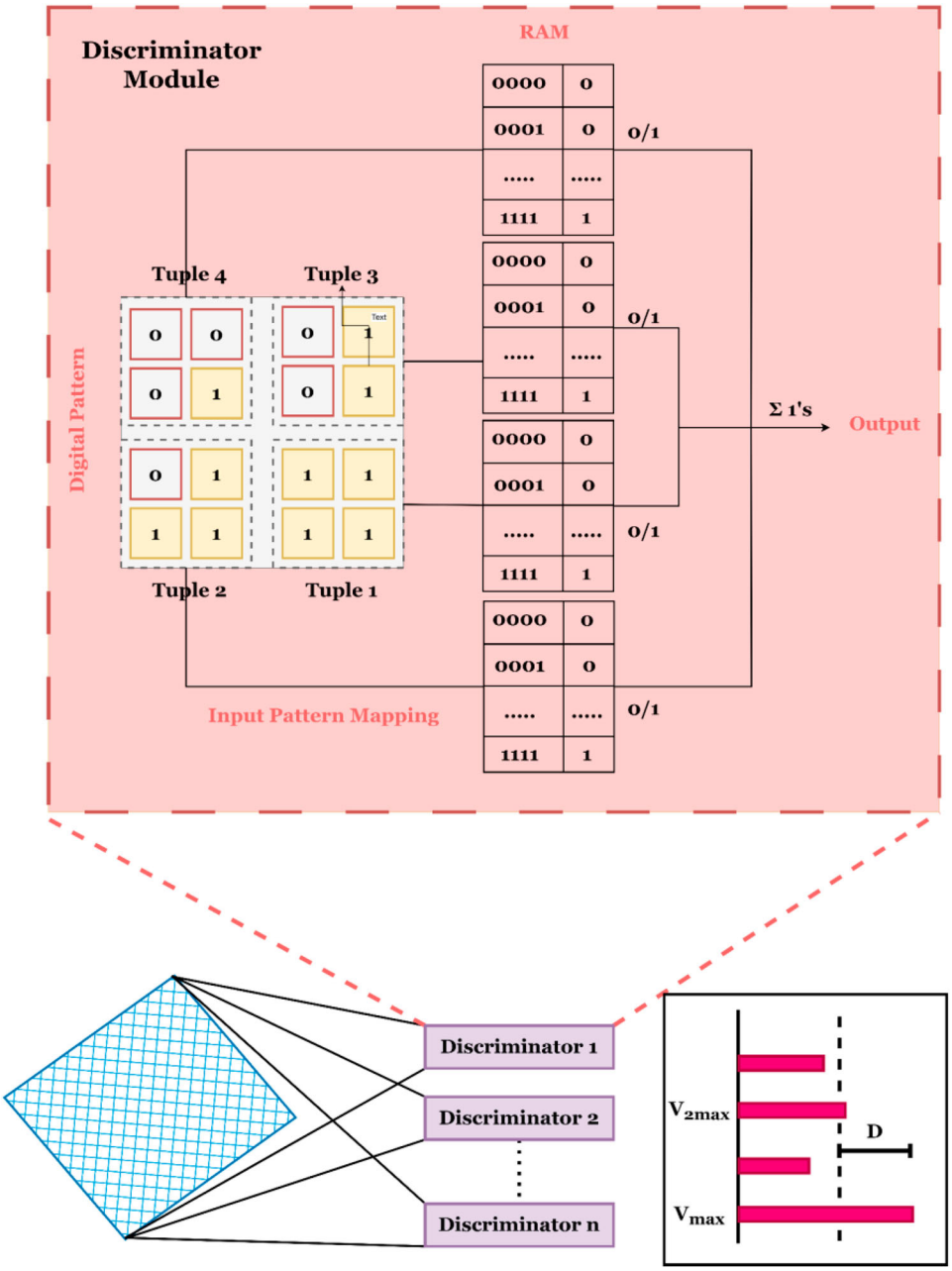

Figure 8. WiSARD classifier with discriminator module.

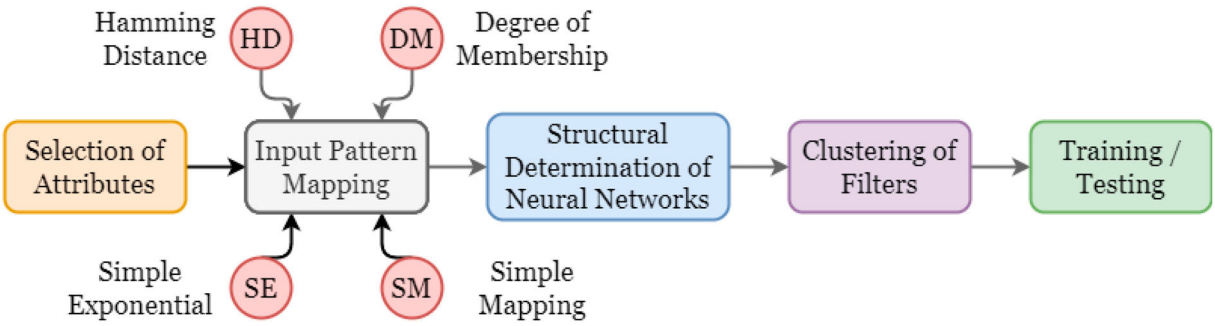

Figure 9. The overall workflow of the WiSARD classifier.

Table 4. Training set accuracy for varying bit numbers.

Hyper-parameter	Statistical features		Histogram features		ARMA features	
Bit no	Accuracy (%)	Time (s)	Accuracy (%)	Time (s)	Accuracy (%)	Time (s)
4	96.87	0.05	93.23	0.07	94.27	0.96
8	100.00	0.02	95.83	0.04	97.39	0.70
16	99.47	0.01	95.83	0.05	97.91	0.60
32	100.00	0.04	95.83	0.03	100.00	0.60

Table 5. Cross-validation accuracy for varying bit numbers.

Hyper-parameter	Statistical features		Histogram features		ARMA features	
Bit no	Accuracy (%)	Time (s)	Accuracy (%)	Bit No	Accuracy (%)	Time (s)
4	81.77	0.01	79.16	0.01	90.62	0.24
8	85.93	0.01	79.68	0.01	92.70	0.14
16	90.10	0.01	79.16	0.01	90.62	0.12
32	88.02	0.01	78.64	0.01	92.70	0.01

Table 6. Test accuracy for varying bit numbers.

Hyper-parameter	Statistical features		Histogram features		ARMA features	
Bit no	Accuracy (%)	Time (s)	Accuracy (%)	Bit No	Accuracy (%)	Time (s)
4	93.75	0.01	87.50	0.01	97.91	0.02
8	97.91	0.01	91.66	0.01	97.91	0.02
16	89.58	0.01	91.66	0.01	100.00	0.02
32	83.33	0.02	91.66	0.01	97.91	0.02

Table 7. Training set accuracy for varying bleach confidence.

Hyper-parameter	Statistical features		Histogram features		ARMA features	
Bleach confidence	Accuracy (%)	Time (s)	Accuracy (%)	Time (s)	Accuracy (%)	Time (s)
0.6	100.00	0.02	95.31	0.06	100.00	0.74
0.7	98.43	0.01	97.39	0.06	98.95	0.80
0.8	100.00	0.05	94.27	0.06	99.47	0.82
0.9	99.47	0.10	96.87	0.06	100.00	0.74
0.95	97.91	0.06	100.00	0.07	98.95	0.78

Table 8. Cross-validation accuracy for varying bleach confidence.

Hyper-parameter	Statistical features		Histogram features		ARMA features	
Bleach confidence	Accuracy (%)	Time (s)	Accuracy (%)	Time (s)	Accuracy (%)	Time (s)
0.6	87.50	0.01	79.68	0.02	92.70	0.20
0.7	86.97	0.02	88.54	0.01	90.62	0.18
0.8	87.50	0.01	86.97	0.01	91.66	0.02
0.9	89.06	0.16	86.45	0.01	89.58	0.02
0.95	88.54	0.01	88.54	0.02	89.58	0.02

Table 9. Test set accuracy for varying bleach confidence.

Hyper-parameter	Statistical features		Histogram features		ARMA features	
Bleach confidence	Accuracy (%)	Time (s)	Accuracy (%)	Time (s)	Accuracy (%)	Time (s)
0.6	91.66	0.02	91.66	0.01	97.91	0.02
0.7	88.54	0.01	97.91	0.02	97.91	0.02
0.8	87.50	0.01	97.20	0.01	100.00	0.02
0.9	89.58	0.01	96.45	0.01	97.91	0.02
0.95	89.58	0.02	95.41	0.02	97.91	0.02

Table 10. Training set accuracy for varying bleach flags.

Hyper-parameter	Statistical features		Histogram features		ARMA features	
Bleach flag	Accuracy (%)	Time (s)	Accuracy (%)	Time (s)	Accuracy (%)	Time (s)
True	90.10	0.14	39.06	0.15	63.02	0.15
False	99.47	0.14	94.15	0.07	100.00	0.07

The impact of bit number on the performance metrics adopted is detailed in Tables 4–6, respectively. The highest value of test accuracy achieved for a particular bit number is identified and revealed as the optimal value. To uphold fairness in the experiment, all remaining parameters were retained at their default settings, except for the bit number. Analysing the outcomes depicted in Table 6 reveals that a bit number of 8 is

Table 11. Cross-validation accuracy for varying bleach flags.

Hyper-parameter	Statistical features		Histogram features		ARMA features	
Bleach flag	Accuracy (%)	Time (s)	Accuracy (%)	Time (s)	Accuracy (%)	Time (s)
True	62.50	0.02	31.25	0.15	61.45	0.02
False	86.97	0.01	88.54	0.07	91.66	0.02

Table 12. Test set accuracy for varying bleach flags.

Hyper-parameter	Statistical features		Histogram features		ARMA features	
Bleach flag	Accuracy (%)	Time (s)	Accuracy (%)	Time (s)	Accuracy (%)	Time (s)
True	79.16	0.02	29.16	0.03	70.83	0.03
False	93.75	0.02	97.91	0.01	100.00	0.02

Table 13. Training set accuracy for varying bleach steps.

Hyper-parameter	Statistical features		Histogram features		ARMA features	
Bleach step	Accuracy (%)	Time (s)	Accuracy (%)	Time (s)	Accuracy (%)	Time (s)
1	99.47	0.12	97.91	0.08	99.54	0.86
2	98.95	0.13	97.39	0.06	99.47	0.74
5	99.47	0.12	98.95	0.05	100.00	0.70
10	98.95	0.10	93.75	0.03	98.43	0.76

Table 14. Cross-validation accuracy for varying bleach steps.

Hyper-parameter	Statistical features		Histogram features		ARMA features	
Bleach step	Accuracy (%)	Time (s)	Accuracy (%)	Time (s)	Accuracy (%)	Time (s)
1	86.97	0.02	87.50	0.01	90.62	0.02
2	88.02	0.13	85.41	0.01	89.58	0.02
5	85.93	0.02	87.50	0.01	92.18	0.02
10	86.97	0.01	85.93	0.01	91.14	0.18

suggested for statistical and histogram features while 16 is suggested for ARMA features.

4.2. Effect of bleach confidence

The confidence in predicting the uniformity among the incoming and stored patterns in the WiSARD classifier is termed bleach confidence. The confidence of the classifier relies on the match-making between the input and stored patterns. Confidence enhances accurate matching and vice versa. The overall prediction accuracy of the classifier accelerates with the improvement in the confidence factor. Tables 7–9 display the tailor-made bleach confidence values used in the study. The findings shown in Table 9 suggest that when employing bleach confidence values of 0.60, 0.70 and 0.80, the WiSARD classifier exhibited improved accuracy for statistical, histogram and ARMA features, respectively.

4.3. Effect of "bleach flag"

The change in prediction confidence is determined by a Boolean indication in the WiSARD classifier with the bleach flag hyperparameter. The confidence value will be altered when the bleach flag value is set to true while no modifications in the confidence value occur when the bleach flag value is set to false. Bleach flag delivers the control on the confidence modification such that the decision-making of the classifier is optimal. Tables 10–12 represent the obtained values for bleach flag variation.

4.4. Effect of "bleach step"

Overfitting in neural networks was widely encountered with the aid of the bleaching process. Such a scenario occurs when the neural network model gains more interest towards the training data. Apart from bleaching, several other techniques such as dropout, regularization, architecture modification and early stopping can be used to control overfitting. The pace of bleaching in the WiSARD classifier is limited by the bleach step hyperparameter. The swiftness of the bleaching process is achieved for higher bleach step values and vice versa. Tables 13–15 provide a unique viewpoint regarding how the bleach step affects the performance metrics.

4.5. Effect of "map type"

The diverse techniques used for associating an input pattern to an individual bit cell of a classifier are handled through a map-type hyperparameter. The distribution of the input data characteristics and the bit cell association are dictated by the map type considered. Linear and random are the two different map types associated with the WiSARD classifier. The former assigns features sequentially, thereby creating a predictable map while the latter randomly disperses

Table 15. Supplied test set accuracy for varying bleach steps.

Hyper-parameter	Statistical features		Histogram features		ARMA features	
Bleach step	Accuracy (%)	Time (s)	Accuracy (%)	Time (s)	Accuracy (%)	Time (s)
1	85.41	0.02	97.91	0.01	95.83	0.02
2	91.66	0.04	100.00	0.01	97.91	0.02
5	95.83	0.02	95.83	0.02	97.91	0.02
10	92.34	0.03	97.91	0.01	95.83	0.02

Table 16. Training set accuracy for varying bleach flags.

Hyper-parameter	Statistical features		Histogram features		ARMA features	
Map type	Accuracy (%)	Time (s)	Accuracy (%)	Time (s)	Accuracy (%)	Time (s)
Random	99.47	0.15	97.39	0.07	100.00	0.74
Linear	98.43	0.08	98.95	0.04	99.47	0.56

Table 17. Cross-validation accuracy for varying bleach flags.

Hyper- parameter	Statistical features		Histogram features		ARMA features	
Map type	Accuracy (%)	Time (s)	Accuracy (%)	Time (s)	Accuracy (%)	Time (s)
Random	85.93	0.18	85.41	0.02	92.18	0.20
Linear	82.81	0.14	80.72	0.02	86.45	0.10

Table 18. Test set accuracy for varying bleach flags.

Hyper-parameter	Statistical features		Histogram features		ARMA features	
Map type	Accuracy (%)	Time (s)	Accuracy (%)	Time (s)	Accuracy (%)	Time (s)
Random	95.83	0.02	100.00	0.12	97.91	0.20
Linear	89.58	0.01	93.75	0.01	93.75	0.16

the features through the introduction of diversity. Map types can significantly impact the classification performance of the WiSARD classifier. The influence of map type is presented in Tables 16–18.

4.6. Effect of "tic number"

The significance of the number of bits contained within individual bit cells becomes clear when considering the concept of the tic number. The tic number plays a pivotal role in determining two essential aspects: memory capacity and resolution. A greater memory capacity (indicated by a higher tic number) results in an expanded memory space within each bit cell, enabling the representation of data patterns in a more aesthetically appealing fashion. Also, the ability of the classifier to represent intrinsic details derived from the input patterns is enhanced with a higher tic number. On the other hand, higher values of the tic number can utilize more memory and increase computational complexity. As a result, the selection of optimal tic number value creates a balance between resolution and memory capacity. Tables 19–21 provide a clear understanding of how the number of tics influences the performance of the WiSARD classifier.

4.7. Optimal hyper-parameter selection

Table 22 provides a visual representation of experiment outcomes, showcasing the selection of optimal hyperparameters, as discussed in previous sections. The data presented in Table 20 emphasizes that by utilizing ARMA features, achieved an impressive 100% classification accuracy. To evaluate the model's performance under these optimal hyperparameter settings, we employed a confusion matrix, as illustrated in Figure 10. A confusion matrix, an essential tool for assessing classification algorithms, provides a comprehensive overview of the algorithm's predictions on a test dataset, allowing for a detailed comparison between predicted and true labels. In this specific multiclass classification scenario, where distinguishing between faulty and non-faulty tires is of utmost importance, the matrix exhibited a remarkable level of precision, with minimal misclassifications. It is worth noting that the testing phase of the model was exceptionally short, with a duration of just 0.02 s, suggesting its potential suitability for present fault diagnosis systems. The current research underscores the crucial importance of the WiSARD classifier configuration, especially when employing 8 bits and 256 tics, in consistently yielding accurate classification results. Furthermore, the research effectively demonstrates the efficiency of the projected fault diagnosis approach with the use of the WiSARD classifier.

4.8. Performance evaluation of the WiSARD classifier with state-of-the-art techniques

The present section elaborates on the superiority of the proposed technique over the state-of-the-art techniques presented in various literature. Table 23 details

Table 19. Training set accuracy for varying tic numbers.

Hyper-parameter	Statistical features		Histogram features		ARMA features	
Tic no	Accuracy (%)	Time (s)	Accuracy (%)	Time (s)	Accuracy (%)	Time (s)
1	25.00	0.01	26.04	0.01	26.04	0.01
10	36.45	0.01	79.16	0.02	82.81	0.02
20	63.54	0.01	81.25	0.01	94.27	0.10
50	83.33	0.01	91.14	0.01	97.91	0.16
100	91.14	0.03	90.05	0.02	99.47	0.30
256	99.47	0.11	98.95	0.07	98.95	0.78

Table 20. Cross-validation accuracy for varying tic numbers.

Hyper-parameter	Statistical features		Histogram features		ARMA features	
Tic no	Accuracy (%)	Time (s)	Accuracy (%)	Time (s)	Accuracy (%)	Time (s)
1	24.47	0.01	25.00	0.01	25.52	0.01
10	34.37	0.02	78.12	0.01	81.25	0.02
20	59.89	0.01	76.56	0.01	89.06	0.20
50	74.47	0.02	80.20	0.02	89.58	0.10
100	78.64	0.01	91.66	0.01	91.14	0.08
256	85.93	0.01	85.41	0.01	92.18	0.02

Table 21. Test accuracy for varying tic numbers.

Hyper-parameter	Statistical features		Histogram features		ARMA features	
Tic no	Accuracy (%)	Time (s)	Accuracy (%)	Time (s)	Accuracy (%)	Time (s)
1	25.00	0.01	25.00	0.22	25.00	0.10
10	27.08	0.02	81.25	0.01	89.58	0.01
20	56.25	0.03	89.58	0.03	95.83	0.02
50	72.91	0.06	97.92	0.08	95.83	0.04
100	75.00	0.01	95.31	0.01	93.75	0.10
256	95.83	0.02	100.00	0.01	100.00	0.02

Table 22. Optimal hyper-parameters of the WiSARD classifier.

Features	Bit number	Bleach confidence	Bleach flag	Bleach step	Map type	Tic number	Accuracy (%)	Time
Statistical	8	0.6	False	5.0	RANDOM	256	95.83	0.02
Histogram	8	0.7	False	2.0	RANDOM	256	97.91	0.01
ARMA	**16**	**0.8**	**False**	**5.0**	**RANDOM**	**256**	**100.00**	**0.02**

Table 23. Comparison with state-of-the-art techniques.

Ref no.	Technique	Accuracy (%)
[28]	K-Star Algorithm	89.16
[29]	CNN	90.00
[30]	Random Forest	90.54
[31]	Long Short-Term Memory Network (LSTM)	83.00
[29]	ResNet	90.00
Proposed	**WiSARD + ARMA**	**100.00**

the performance evaluation of the proposed WiSARD approach.

5. Conclusion

The present study was formulated to monitor the condition of nitrogen-filled tires at four different conditions namely, high, puncture, idle and normal using vibration analysis and the WiSARD classifier. The vibration data for every tire condition were extracted from the nitrogen-filled tire using a MEMS accelerometer attached to the rear axle. Essential features such as ARMA, histogram and statistics were extracted from the raw data and significant features were selected using the J48 algorithm. The selected features were split into training and testing datasets. The performance of the WiSARD classifier was assessed for various hyperparameters such as tic number, bit number, bleach confidence, map type, bleach flag and bleach step, respectively. The obtained results were analysed and the optimal hyperparameters were selected for every feature. The results obtained inferred that a maximum classification accuracy of 100.00% was achieved for ARMA features with optimal hyperparameter settings. Based on the insights gained, it can be inferred that the utilization of the WiSARD classifier in conjunction with ARMA features offers a promising method for examining TPMS nitrogen vibration data. The following conclusion can be derived based on the findings presented above.

- The study demonstrates that utilizing the WiSARD classifier in conjunction with ARMA features resulted in a maximum classification accuracy of 100.00%. This success implies the effectiveness of this approach in accurately monitoring nitrogen-filled tire conditions under various scenarios such as high stress, puncture, idle and normal conditions.

Nitrogen Filled Tire Condition Monitoring - ARMA Features					
TARGET / OUTPUT	High	Normal	Puncture	Idle	SUM
High	12 25.00%	0 0.00%	0 0.00%	0 0.00%	12 100.00% 0.00%
Normal	0 0.00%	12 25.00%	0 0.00%	0 0.00%	12 100.00% 0.00%
Puncture	0 0.00%	0 0.00%	12 25.00%	0 0.00%	12 100.00% 0.00%
Idle	0 0.00%	0 0.00%	0 0.00%	12 25.00%	12 100.00% 0.00%
SUM	12 100.00% 0.00%	12 100.00% 0.00%	12 100.00% 0.00%	12 100.00% 0.00%	48 / 48 100.00% 0.00%

Figure 10. Confusion matrix of the WiSARD classifier for ARMA features.

- The research identifies and selects optimal hyperparameter settings for the WiSARD classifier, considering parameters such as tic number, bit number, bleach confidence, map type, bleach flag and bleach step. This finding is crucial as it enhances the understanding of how tuning these hyperparameters contributes to achieving the highest classification accuracy, providing valuable insights for future applications.
- The study suggests that the combination of the WiSARD classifier and ARMA features presents a promising method for analysing Tire Pressure Monitoring System (TPMS) nitrogen vibration data. This conclusion implies that this approach can be a reliable and effective tool for monitoring and assessing the condition of nitrogen-filled tires, offering potential applications in the field of automotive safety and maintenance.
- The findings of the study not only showcase high classification accuracy but also underscore the viability of real-time deployment for monitoring nitrogen-filled tire conditions. The successful integration of the WiSARD classifier with ARMA features suggests that this methodology can be implemented in real-world scenarios, providing instantaneous feedback on tire health.
- By continuously monitoring nitrogen-filled tire conditions, the proposed methodology could contribute to the early detection of potential tire failures or deviations from normal operating conditions. This proactive approach improves overall vehicle safety.
- The study bridges the gap between advanced data analytics and practical automotive maintenance. This intersection holds promise not only for vehicle manufacturers and fleet managers but also for individuals keen on adopting cutting-edge technology to ensure the reliability and safety of their vehicles.

Disclosure statement

No potential conflict of interest was reported by the author(s).

Data availability statement

The datasets generated and/or analysed during the current study are available from the corresponding author upon reasonable request.

Funding

No funding was received for the research work carried out.

ORCID

V. Sugumaran http://orcid.org/0000-0002-5323-6418

References

[1] Lee H, Taheri S. Intelligent tires-a review of tire characterization literature. IEEE Intell Transp Syst Mag. 2017;9:114–135. doi:10.1109/MITS.2017.2666584

[2] Pardeshi SS, Patange AD, Jegadeeshwaran R, et al. Tyre pressure supervision of two wheeler using machine learning. SDHM Struc Durabil Health Monit. 2022;16:271–290.

[3] Haq MT, Zlatkovic M, Ksaibati K. Assessment of tire failure related crashes and injury severity on a mountainous freeway: Bayesian binary logit approach. Accid Anal Prev. 2020;145.
[4] Vasan V, Sridharan NV, Prabhakaranpillai Sreelatha A, et al. Tire condition monitoring using transfer learning-based deep neural network approach. Sensors. 2023;23. doi:10.3390/s23042177
[5] Jatakar KH, Mulgund GV, Patange AD, et al. Two-wheeler tyre pressure monitoring through K-nearest neighbours algorithm trained using wheel hub vibrations acquired using ADXL335 accelerometer. Int J Veh Noise Vib. 2022;18. doi:10.1504/IJVNV.2022.128286
[6] Lee DH, Yoon DS, Kim GW. New indirect tire pressure monitoring system enabled by adaptive extended kalman filtering of vehicle suspension systems. Electronics (Switzerland). 2021;10:1–19. Article number 1359.
[7] Silalahi LM, Alaydrus M, Rochendi AD, et al. Design of tire pressure monitoring system using a pressure sensor base. Sinergi. 2019;23. doi:10.22441/sinergi.2019.1.010
[8] Hasan NN, Arif A, Pervez U. Tire pressure monitoring system with wireless communication. Canadian Conference on Electrical and Computer Engineering; 2011.
[9] Wei C, Zhou W, Wang Q, et al. TPMS (tire-pressure monitoring system) sensors: monolithic integration of surface-micromachined piezoresistive pressure sensor and self-testable accelerometer. Microelectron Eng. 2012;91:167–173.
[10] Patil RR, Shinde AA. Wireless tyre pressure measurement. Indian J Sci Technol [Internet]. 2021;14:842–849. doi:10.17485/IJST/v14i9.2296. Available from: https://indjst.org/articles/wireless-tyre-pressure-measurement.
[11] Caban J, Droździel P, Barta D, et al. Vehicle tire pressure monitoring systems. Diagnostyka. 2014;15:11–14.
[12] Szczucka-Lasota B, Kaminska J, Krzyzewska I. Influence of tire pressure on fuel consumption in trucks with installed tire pressure monitoring system (TPMS). Sci J Silesian Univ Technol Ser Transport. 2019;103. doi:10.20858/sjsutst.2019.103.13
[13] Wei L, Wang X, Li L, et al. A low-cost tire pressure loss detection framework using machine learning. IEEE Trans Ind Electron. 2021;68:12730–12738.
[14] Muturatnam AB, Sridharan NV, Sreelatha AP, et al. Enhanced tyre pressure monitoring system for nitrogen filled tyres using deep learning. Machines. 2023;11. doi:10.3390/machines11040434
[15] Pardeshi SS, Patange AD, Jegadeeshwaran R, et al. Tyre pressure supervision of two wheeler using machine learning. SDHM Struct Durabil Health Monit. 2022;16:271–290.
[16] Anoop PS, Sugumaran V, Mithun Praveen H. Implementing K-star algorithm to monitor tyre pressure using extracted statistical features from vertical wheel hub vibrations. Indian J Sci Technol. 2016;9. doi:10.17485/ijst/2016/v9i47/107926
[17] Chuntama T, Techa-Angkoon P, Suwannajak C, et al. Multiclass classification of astronomical objects in the galaxy M81 using machine learning techniques. 2020 24th International Computer Science and Engineering Conference, ICSEC 2020; 2020.
[18] De Souza AF, Freitas FD, De Almeida AGC. High performance prediction of stock returns with VG-RAM weightless neural networks. Proceedings of the 3rd Workshop on High Performance Computational Finance, WHPCF 2010; 2010.
[19] Cardoso D, De Gregorio M, Lima P, et al. A weightless neural network-based approach for stream data clustering. Lecture Notes in Computer Science (including subseries Lecture Notes in Artificial Intelligence and Lecture Notes in Bioinformatics); 2012.
[20] McElroy B, Howells G. Automated adaptation of input and output data for a weightless artificial neural network. Int J Database Theory Appl. 2011;4:49–58.
[21] Subhashini R, Nagarajan E, Niveditha PR. Detection of an incognitos intruder in industries and semantic mapping of emotions. Int J Appl Eng Res. 2014;9:6727–6734.
[22] Lacerda Queiroz R, Ferrentini Sampaio F, Lima C, et al. AI from concrete to abstract: demystifying artificial intelligence to the general public. AI Soc. 2021;36. doi:10.1007/s00146-021-01151-x
[23] Aleksander I, Thomas W V, Bowden PA. Wisard a radical step forward in image recognition. Sens Rev. 1984:120–124.
[24] Aravinth S. Air compressor fault diagnosis through vibration signals using statistical features and J48 algorithms. Indian J Sci Technol. 2016;9. doi:10.17485/ijst/2016/v9i47/107912
[25] De Gregorio M, Giordano M. The WiSARD classifier. ESANN 2016 – 24th European Symposium on Artificial Neural Networks; 2016.
[26] Sridharan NV, Joseph JV, Vaithiyanathan S, et al. Weightless neural network-based detection and diagnosis of visual faults in photovoltaic modules. Energies (Basel) [Internet]. 2023;16:5824. doi:10.3390/en16155824
[27] Chan D, Hockaday S, Tillett RD, et al. Factors affecting the training of a WISARD classifier for monitoring fish underwater. British Machine Vision Association and Society for Pattern Recognition; 2013. p. 34.1–34.12.
[28] Anoop PS. Implementing K-star algorithm to monitor tyre pressure using extracted statistical features from vertical wheel Hub vibrations. Indian J Sci Technol. 2016;9:1–7. doi:10.17485/ijst/2016/v9i47/107926
[29] Ziaukas Z, Busch A, Wielitzka M, et al. Classification of tire pressure in a semitrailer using a convolutional neural network. 2020 IEEE International Conference on Mechatronics and Automation (ICMA). IEEE; 2020. p. 181–185.
[30] Svensson O, Thelin S, Byttner S, et al. Indirect tire monitoring system – machine learning approach. IOP Conf Ser Mater Sci Eng. 2017;252:012018. doi:10.1088/1757-899X/252/1/012018
[31] Wang X, Chen Z, Cao W, et al. Artificial neural network-based method for identifying under-inflated tire in indirect TPMS. IEEE Access. 2020;8:213799–213805. doi:10.1109/ACCESS.2020.3038895